Analytical Methods

Accepted Manuscript

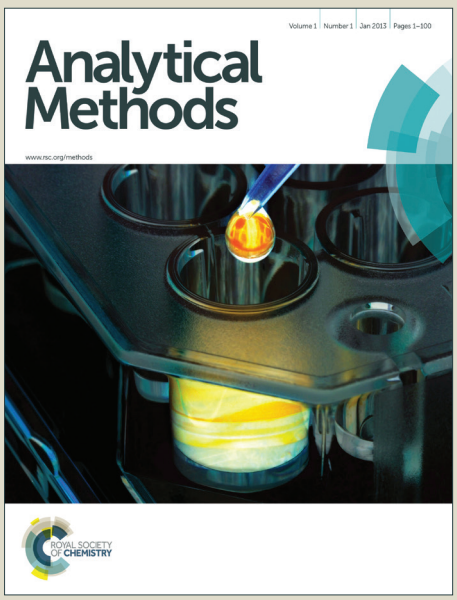

ROYAL SOCIETY OF CHEMISTRY

www.rsc.org/methods

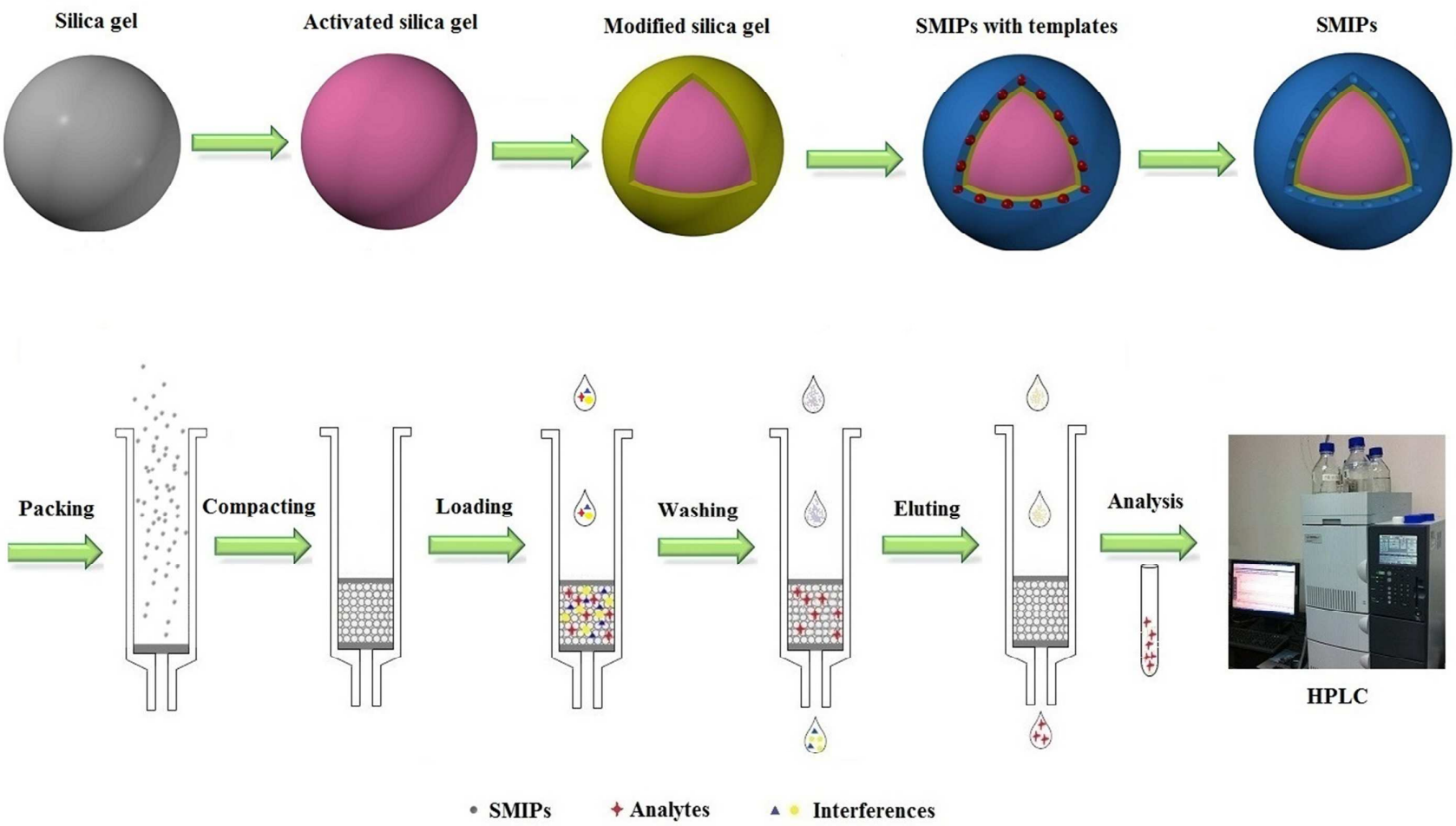

The schematic representation of the route for the synthesis of SMIPs and the analysis of samples

Preparing surface molecularly imprinted polymers as the solid-phase extraction sorbents for the specific recognition of penicilloic acid in penicillin

Zhimin Luo, Aiguo Zeng, Penglei Zheng, Pengqi Guo, Wei Du, Kangli Du, Qiang Fu*

Abstract

A method coupling SMIPs-SPE with high-performance liquid chromatography (HPLC) was established for the detection of the trace amount of PNLA in penicillin. Highly selective surface molecularly imprinted polymers (SMIPs) for penicilloic acid were prepared and used as solid-phase extraction sorbents for the specific recognition, enrichment, extraction and detection of penicilloic acid (PNLA) in penicillin. The polymers were characterised in terms of their physical and morphological properties by using SEM, FTIR, thermo gravimetric analyses, nitrogen adsorption and desorption analyses and elemental analyses. The adsorption properties of the products obtained were studied, including the adsorption of isotherms, kinetics and selectivity. The results demonstrated that SMIPs possess a high adsorption capacity, rapid mass-transfer rate and high selectivity to PNLA when compared with non-imprinted polymers (SNIPs) and bulk molecularly imprinted polymers (MIPs). SMIPs adopted as the sorbents of solid-phase extraction (SMIPs-SPE) were used to extract the penicilloic acid from the parent drug, the reusability and stability of which were investigated. The results of the method validation showed that the intra-day and inter-day accuracy were ≥ 93.2% and ≥ 90.9%, respectively. The RSD% of

* *School of Pharmacy, Xi'an Jiaotong University, 76 Yanta West Street, Xi'an, 710061, PR China. E-mail: fuqiang@mail.xjtu.edu.cn; Fax: +86 82655382.*

repeatability ranged from 0.7% to 6.8%, and that of the intermediate precision ranged from 4.9% to 7.4%. The limit of detection (LOD) and the limit of quantitation (LOQ) were 0.03 mg g^{-1} and 0.1 mg g^{-1}, respectively. This work provides a promising method for monitoring the allergenic impurity in penicillin and improving the purity of penicillin.

Introduction

Impurities in pharmaceuticals are unwanted chemicals that coexist with active pharmaceutical ingredients. The presence of these related substances, even in small amounts, may influence the efficacy and safety of the pharmaceutical products. Therefore, the control of pharmaceutical impurities is currently a critical issue for the pharmaceutical industry[1].

Penicillin is an important β-lactam antibiotic that made a significant breakthrough in fighting infectious disease during the Second World War[2]. Today, penicillin remains a first-line antibiotic, which is efficient against a number of different types of infections and is widely used in developing counties. However, approximately 10% of hospitalised patients have allergic reaction[3,4] (e.g. rash, urticaria, wheezing and anaphylactic shock). The causative factors for eliciting allergic reactions have been studied extensively for penicillin, and it has been reported that the impurities of penicillin induced the anaphylactic reaction[5-9]. These allergenic impurities consist of macromolecular impurities (such as penicilloyl-proteins[10], penicilloyl-peptides[11] and oligomers[12,13]) and relatively small molecular impurities (such as penicilloic acid[5], penicillenic acid[7]). Almost all of macromolecular impurities

can be eliminated by protein precipitation, solvent extraction or column chromatography[2,14]. However, small molecular impurities are difficult to be removed from parent drug because of the similarity of their basic structures and their analogous chemical properties. Therefore, it is essential to monitor these relatively small molecular impurities. Because of the lack of impurity reference substance, the relatively small molecular impurities cannot be effectively controlled, and the main component self-compare is just used to monitor each untargeted impurity of penicillin in pharmacopoeia of many countries (MRL ≤ 0.1 mg g^{-1}), including the European Pharmacopoeia 7.0 [15], the Japanese Pharmacopoeia [16] and the Pharmacopoeia of the People's Republic of China [17]. Up to now, few studies reported about the enrichment, extraction and detection of these relatively small molecular impurities in penicillin. More seriously, there exists a similar situation in other useful β-lactam antibiotics[18].

Penicilloic acid (PNLA), as a antigenic determinant, takes an important responsibility for the allergenicity of penicillin, because it can bind covalently to macromolecular carriers in the body, eliciting sensitising conjugates [5,9,11,13]. During the procedure of production, storage, transportation and use of penicillin, a small amount of penicillin is prone to be decomposed into PNLA [9,18]. Therefore, the control of penicilloic acid is a critical issue for the quality control of penicillin. To the best of our knowledge, there is no research published to date on separating or removing the relatively small molecular impurity penicilloic acid from penicillin. A number of articles have described the determination of penicilloic acid in penicillin using

mercurimetric titration[19], iodometric assay[20], the colorimetric method[21] and thin-layer chromatography[22]. Nevertheless, these methods have poor accuracy, complicated steps and time-consuming. Therefore, the need for a fast, sensitive, simple and selective method is obvious, especially for the quantity control of penicilloic acid.

Currently, solid-phase extraction is used to remove the interferents and concentrate the target analytes. Therefore, it is widely used in the fields of enrichment, extraction and purification[23]. However, the universal SPE sorbent is n-alkylsilica (C8 and C18), which suffers from the low selectivity and poor recovery for target analytes. Consequently, specific recognition adsorbents for SPE use are in demand.

Molecular imprinting is a template polymerisation technique for producing complementary binding sites with specific compound recognition ability[24,25]. Because of its simple preparation method, good stability and excellent recognition properties, molecularly imprinted polymers (MIPs) have been widely used as SPE sorbents in the areas of biological analysis[26,27], residue detection[28], phytoextraction[29,30,31], trace element detection[32] and genotoxicity removement[33,34]. Conventional MIPs prepared by bulk polymerisation show remarkable imprinting properties but with low capacity and poor site accessibility to target analytes[35]. This is attributed to the highly cross-linked nature of MIPs that templates embedded deeply inside the thick polymer network and cause the difficulty of removal of the templates. In contrast, the surface imprinting technique can generate enough cavities at the surface or close to the materials' surface. This merit facilitates fast mass transfer, rapid binding kinetics and

more accessible binding sites[36]. Accordingly, it is possible that surface molecularly imprinted polymers (SMIPs) function better than conventional MIPs as truly robust and rigid stationary sorbents for the specific recognition of target analytes.

In this work, molecular imprinting technology is firstly used in the control of the impurities of penicillin. SMIPs-SPE coupled with HPLC was used for the selective recognition, enrichment and detection of penicilloic acid in penicillin. Surface molecularly imprinted polymers were prepared as SPE sorbents that could extract or remove penicilloic acid from the parent drug. At the same time, the surface molecularly imprinted polymers were compared with the conventional MIPs.

Experimental

Chemicals and materials

Penicilloic acid and cloxacilloic acid (CLA) were synthesised following a previously described procedure[37]. The solid raw medicines penicillin G (PENG)(≥98%), 6-aminopenicilanic acid (6-APA)(≥99%), benzoic acid (BA) (≥95%), and oxiracetam (OXRT) (≥94%) were purchased from Xi'an Renda Biotechnology Co. (Xi'an, China). Five batches of benzylpenicillin sodium for injection were purchased from Ⅰ: Harbin Pharmaceutical Group Co., Ltd. (8×10^5 IU, batch lot: A110300515), Ⅱ: Youcare Pharmaceutical Group Co., Ltd. (8×10^5 IU, batch lot: 1111091), Ⅲ: Shandong Lukang Pharmaceutical Group Co., Ltd. (8×10^5 IU, batch lot: L110943), Ⅳ: Shandong Lukang Pharmaceutical Group Co., Ltd. (16×10^5 IU, batch lot: S111038), and Ⅴ: Shandong Lukang Pharmaceutical Group Co., Ltd. (8×10^5 IU, batch lot: B111108), respectively. Methacrylic acid (MAA) was purchased

from Tianjin Chemical Reagent Plant (Tianjin, China). Ethylene glycol dimethacrylate (EGDMA) was obtained from Sigma-Aldrich (New Jersey, USA). The molecule 2,2'-azobis(2-methylpropionitrile) (AIBN) was purchased from Shanghai No.4 Reagent Factory (Shanghai, China) and recrystallised in methanol before use. The molecules 3-aminopropy-ltriethoxysilane (APTES) and triethylamine were obtained from J&K Scientific LTD (Peking, China). Acetonitrile and methanol were of HPLC grade, purchased from Kemite Co. (Tianjin, China). Silica gels were obtained from Tokyo Chemical Industry, Ltd. (average diameter: 100 μm, Tokyo, Japan). Ultra-pure water was purified with Molement 1805b (Shanghai, China). Toluene was of analytical grade and supplied by local suppliers. All other chemicals were of analytical grade and supplied by local suppliers. Empty SPE cartridges (10 mL) were obtained from Shenzhen Doudian Co. (Shenzhen, China).

Chromatographic conditions

The HPLC analysis was performed with a Shimadzu HPLC system (LC 2010A HT, Kyoto, Japan), equipped with a LC-2010A HT pump, a SPD-20A UV-vis detector and a CBM-102 work station; a Promosil C18 column (150×4.6mm, i.d. 5 μm) was used for analysis. The mobile phase consisted of acetonitrile/diammonium phosphate (0.05 mol L^{-1}) (15:85, v/v) and the pH of the mobile phase was 6.18, which was checked by Mettler Toledo pH-meter (Shanghai, China). The wavelength of the ultraviolet detector was 230 nm. The injection volume was 10 μL, and the column temperature was maintained at 30 ℃.

Preparation of the polymers

The schematic route for the preparation of SMIPs is shown in Figure 1.The preparation of the SMIPs is as follows[38].

Silica gels (30 g) were dispersed in a 10% hydrochloric acid solution (250 mL) with stirring, and they were refluxed at 110 ℃ for 24 h. The obtained particles were filtered and washed with ultra-pure water to neutral, and then the activated silica gels were dried at 60 ℃ for 24 h. The activated silica gels (10 g), APTES (4 mL) and triethylamine (2 mL) were dispersed in 100 mL of toluene with stirring, and were refluxed for 24 h at 110 ℃. The products (APTES-SiO2) were filtered and washed with methanol and dried at 60 ℃ for 24 h. The obtained APTES-SiO_2 were dispersed in methanol (10 mL) and acetonitrile (10 mL). PNLA (176.2 mg, 0.5 mmol) as the template and MAA (168 μL, 2 mmol) as the functional monomer were added and dissolved in the above solution for prepolymerisation for approximately 15 h. Then, EGDMA (952 μL, 5 mmol) as the cross-linker and AIBN (16.4 mg) as the initiator were added and dissolved for polymerisation at 60 ℃ for 24 h. The products were filtered and washed with methanol (100 mL). Afterward, PNLA was removed by Soxhlet extraction with 100 mL of methanol and acetic acid (4:1, v/v) for 48 h. Then, the products were washed with 200 mL of acetonitrile and water (1:9, v/v) until neutrality. The obtained SMIPs were filtered, washed with 50 mL of methanol and dried under vacuum at 60 ℃ for 24 h by using Vacuum freeze dryer purchased from Xiamen Lianyou Refrigeration Equipments Co. Ltd. (Xiamen, China).

Non-imprinted polymers (SNIPs) were prepared in the same way as for SMIPs

but without the addition of the template molecules. The bulk molecularly imprinted polymers (MIPs) were fabricated identically but without the support of silica gels.

Characterisation of the polymers

The morphology of the activated silica gels, SMIPs and SNIPs were observed by a TM-1000 Scanning Electron Microscope (SEM) (Hitachi, Japan).

Fourier transform infrared spectra (FTIR) were recorded on a Thermo Nicolet Nexus 330 FT-IR spectrometer (Madison, USA) with a scanning range from 400 to 4000 cm^{-1}.

Thermo gravimetric analyses (TGA) were performed simultaneously using a SDT Q600 thermogravimetric analyser (TA, New Castle, USA).

Nitrogen adsorption and desorption analyses were performed on an Autochem ii 2920 (Quantachrome, USA) with a bath temperature of 77 K. The specific surface area (S) was determined using the Brunauer-Emmett-Teller (BET) theory; the average pore diameter (d_p) and the specific pore volume (V_p) were calculated from the nitrogen adsorption and desorption isotherms using the Barrett-Joyner-Halenda (BJH) theory.

Elemental analyses were obtained by an EL3 elementary analyser (Elementer, Germany). The parameters are calculated as follows[24].

The area density (D) is calculated from the increase in the carbon content after the corresponding coupling as[24],

$$D = \frac{m_x}{M_x \times S} \quad , \tag{1}$$

$$m_x = \frac{X\%}{\left(100 - \frac{X\% \times M_w}{M_x}\right)} \quad , \tag{2}$$

where M_w = molecular weight of the immobilised silane, M_x = weight of carbon (X=C) per mole of immobilised species, and S = surface area of the silica support.

Coverage (C) is calculated as[24],

$$C = \frac{100 \times D}{8} \quad , \tag{3}$$

assuming a maximum silanol group density of 8 μmol·$(m^2)^{-1}$.

The average distance (d_L) between the coupled ligands, assuming a random ligand distribution, is calculated as[24],

$$d_L = \sqrt{\frac{10^{18}}{D \times 10^{-6} \times N}} \quad , \tag{4}$$

where N is Avogadro's number.

Film thickness (d) is estimated from the carbon content of the grafted film[24];

$$d = \frac{m_c \times M_w}{M_c \times \rho \times S} \times 10^3 \quad , \tag{5}$$

$$m_c = \frac{\%C}{100 - \left(\frac{\%C \times M_w}{M_c}\right)} \quad , \tag{6}$$

where m_c = weight of carbon of the grafted polymer per gram of bare silica support, Mw = weighted average molecular weight of the grafted polymer assuming stoichiometric incorporation of the reactive monomers, M_C = weighted average molecular weight of the carbon fraction of the grafted polymer, ρ = weighted average density of the monomers (g mL^{-1}) and S = specific surface area of the bare silica support (m^2 g^{-1}).

Adsorption test

To measure the adsorption capacity of SMIPs, PNLA solutions with various concentrations were prepared as extracted samples. The adsorption isotherms were obtained by suspending 20 mg of SMIPs in 10 mL of various PNLA concentrations

(10 to 800 μg·mL^{-1}) at 25 ℃. The adsorption kinetics curves were obtained by detecting the temporal evolution of the PNLA concentration (400 μg·mL^{-1}) in the solutions. The binding amount of PNLA on the SMIPs was determined by the difference between the total PNLA amount and the residual amount in the solutions with the HPLC system. The adsorption capacity Q (mg g^{-1}) was calculated according to the equation as follows.

$$Q = \frac{(C_0 - C_f)v}{m}, \quad (7)$$

where C_0 (μg·mL^{-1}) and C_f (μg·mL^{-1}) are the initial and final concentrations of PNLA in solution, respectively, v (mL) is the total volume of the solution, and m is the mass of SMIPs.

The equilibrium data for PNLA on SMIPs were also modeled with the Freundlich equation (Eq.8) [39] and Langmuir equation (Eq.9)[40].

$$\ln q_e = \ln K_f + \frac{1}{n \ln C_e} \quad (8)$$

$$\frac{1}{q_e} = \frac{1}{K_a q_m C_e} + \frac{1}{q_m} \quad (9)$$

where C_e (μg·mL^{-1}) is the equilibrium concentration of penicilloic acid; q_e (μg·mg^{-1}) is the amount of PNLA adsorbed at equilibrium; K_f and n are the Freundlich constants related to adsorption capacity and adsorption intensity, respectively[39]; and q_m and K_a is the Langmuir constants, which are indictors of adsorption capacity and energy of adsorption, respectively[40].

The competitive adsorption was evaluated among four structural homologues (6-APA, BA, CLA and PENG) and a non-homologue (OXRT). PNLA and 6-APA were all impurities of penicillin[41], so we also attempted to obtain the adsorption

capacity of SMIPs for 6-APA in PENG. Experimental conditions: the concentration of each solution, the volume of each solution, the mass of polymer and the adsorption time were 300 μg·mL^{-1}, 10 mL, 20 mg and 45 min, respectively.

Additional competitive adsorption was evaluated with the mixed solutions of PNLA and its parent medicine (PENG) at four ratios of concentration (9:1, 5:5, 1:9 and 1:99). The experimental conditions were as above but using the mixed solution as the extracted sample. The adsorption ratio (*R*) is calculated according to the equation as follows.

$$R = \frac{(C_0 - C_f)}{C_0} \times 100\% \ , \qquad (10)$$

where C_0 (μg·mL^{-1}) and C_f (μg·mL^{-1}) are the initial and final concentrations of PNLA (or PENG) in the mixed solution, respectively. *R* is the adsorption ratio of PNLA (or PENG) in mixed solution.

SMIPs-SPE conditions

SMIPs weighting 100 mg were dry-packed in an empty SPE cartridge (2.5 mL) between two glass wool frits, and the resulting SPE cartridge was termed SMIPs-SPE. After being activated by 2 mL of ultra-pure water and 1 mL of methanol, the penicillin solutions mixed with PNLA were loaded. Then, the cartridge was washed and eluted with 2 mL of methanol-acetic acid (99:1, v/v) (pH = 5.19) and 4 mL of methanol-acetic acid (9:1, v/v), respectively. The eluent was evaporated under a nitrogen stream, and the residues were redissolved in 1 mL of the mobile phase for analysis.

Method validation

The developed SMIPs-SPE method coupled with HPLC for PNLA analysis was then validated following the recommendations of the International Conference on Harmonization Q2(R1)[42]. Aliquots of the penicillin solution were spiked with various volumes of PNLA solution to obtain various spiked penicillin solutions, of which the concentration of PNLA corresponding to 0.1, 1.0, 5.0, 10, 25, and 50 mg g^{-1}. The linearity of the calibration curve was evaluated for PNLA over the range of 0.1 to 50 mg g^{-1} in penicillin. The method limit of detection (LOD) and limit of quantitation (LOQ) were defined as three and ten times the ratio of the signal to noise, respectively. The accuracy was expressed as a percentage of the recovery. The precision was evaluated by measuring the relative standard deviation (RSD) of the intra-day and inter-day data, with acceptable values for the RSD% being less than 15%[25].

Application

Five batches of aqueous solutions of benzylpenicillin sodium for injection (I~V, 100 μg·mL^{-1}) were detected by HPLC. The mobile phase and the solution of pencilloic acid (100 μg·mL^{-1}) were also injected into the HPLC for analysis as the reference substance. The five batches of benzylpenicillin samples were extracted by SMIPs-SPE, and then the extractions were redissolved and analyzed by HPLC. One of benzylpenicillin sodium solution (100 μg·mL^{-1}) was detected with various placing times at room temperature (0 d, 1 d, 2 d, 3 d, 5 d, 8 d and 10 d, respectively).

Results and discussion

Characterisation of the polymers

The morphology of (a, d) activated silica gels, (b, e) SNIPs and (c, f) SMIPs are shown in Figure 2 with various magnifications. The surfaces of the SNIPs and SMIPs (Figure 2e and f) were much more scabrous than that of the activated silica gels (Figure 2d). Moreover, the size of the SMIPs and SNIPs were larger than that of the activated silica gels, illustrating that the grafted particles were grown onto the surface of the activated silica gels and presented a certain thickness (the diameters of them were all around 100 μm). Additionally, the surface of the SNIPs was much denser than that of SMIPs, and this structure hindered the access of templates.

The FTIR spectra of the activated silica gel particles, APTES-SiO_2, MIPs and SMIPs are shown in Figure 3a, b, c and d, respectively. The bands at 3461 and 1635 cm^{-1} were both attributed to the characteristic vibrational absorption of O-H on the surface of the activated silica gels (Figure 3a) [36]. In Figure 3b, the vibrational absorption of O-H disappeared, and the vibrational absorptions of C-N and N-H appeared at 1096 and 3446 cm^{-1}, respectively, indicating that the silica gels have been successfully modified by APTES. Figure 3c shows the spectrum of MIPs, in which the band at 1097 cm^{-1} was due to the bending vibration of the C-O group, and the peaks at 1558 and 1732 cm^{-1} were the bending vibration of the C=O group [35]. In Figure 3d, the peaks at 1563, 1641 and 1727 cm^{-1} were all attributed to the stretching and bending vibration of the carboxyl or C=O group, and the band at 2970 cm^{-1} was the bending vibration of the methyl group. The peaks at 1109 and 3465 cm^{-1} were the

bending vibration of the Si-O and SiO-H groups[36], respectively, which do not appear in Figure 3c. All of these indicated that the monomer MAA and the cross-linking agent EGDMA were grafted onto the surface of the silica gels and that the fabrication procedure has been successfully performed.

The thermal decomposition of the activated silica gels, APTES-SiO_2, SMIPs and SNIPs were tested (Figure 4). The activated silica gels had only 7% weight loss at 100 ℃, which corresponds to the release of physically adsorbed water. The loss of water exists in all samples. The weight loss of APTES-SiO_2 was approximately 11%. It had a sharp decrease at approximately 300-600 ℃, corresponding to the temperature of decomposition and ashing, and the weight loss of this stage was approximately 4%, in keeping with the weight of the grafted APTES. There was a resemblance between the SMIPs and SNIPs; except for the identical loss of water at approximately 100 ℃, the SMIPs and SNIPs were stable within 300 ℃, which is a benefit for the SMIPs being used as adsorption sorbents. Afterward, they all had a steep loss at approximately 300-450 ℃, corresponding to the degradation of the grafted particles, and the weight losses of the SMIPs and SNIPs were 29% and 38%, respectively. They were both more than that of APTES-SiO_2 (11%), indicating that the monomers and cross-linking agents were grafted onto the surface of the silica gels. However, the weight loss margin between the SMIPs and SNIPs was approximately 9%, and this could be caused by the removal of the template in the SMIPs after polymerisation. Because SNIPs did not contain the template, the surface of the SNIPs was much more compacted than that of the SMIPs. This result corresponds with the

result of SEM.

Nitrogen adsorption and desorption isotherms are informative of the homogeneity of the grafted polymer films[24]. The isotherms for activated silica gels and SMIPs were all type IV curves exhibiting a hysteresis loop (Supplementary information Fig. 1), which indicated homogeneous mesoporosity. This result indicated that the surface of SMIPs was loose and porous. This construction was in favour of the templates moving in and out of the surface of SMIPs. The parameters of the microscopic pore structure are shown in Table 1. The S, d_p and V_p of SMIPs were 264.22 m^2 g^{-1}, 4.93 nm and 0.41 mL g^{-1}, respectively, which were lower than those of activated silica gels, indicating that the attachments were packed in the mesopores or adhered onto the surface of the silica gels. In contrast, the parameters of SMIPs were all higher than those of the SNIPs (236.18 m^2 g^{-1}, 4.28 nm and 0.29 mL g^{-1}, respectively), demonstrating that the SMIPs had more mesopores and were much looser than the SNIPs. Consequently, the SMIPs could provide more accessible three-dimensional cavities for target analytes than SNIPs.

The elemental contents of various samples were investigated by elemental-analysis experiments. As shown in Table 1, carbon and nitrogen appeared in the modified silica gels and imprinted polymers, demonstrating that particles were successfully grown onto the surface of silica gels. The parameters D, C and d increased gradually, whereas d_L decreased successively following the assembling step, namely from the active silica gels, the modified silica gels and the SMIPs. The d and d_L of SMIPs were 2.17 and 0.70 nm, respectively, indicating that the surface of SMIPs

was highly conglomerated and irregularly shaped with particle sizes in nanometres. The *D* and *C* of SMIPs (3.35 μmol·$(m^2)^{-1}$ and 41.82%, respectively) were lower than those of SNIPs (4.57 μmol·$(m^2)^{-1}$ and 57.13%, respectively), whereas the d_L was the opposite, which intuitively-reflected that SMIPs could provide target molecules more steric manoeuvrability within the pore, which led to a higher binding of the template than SNIPs. This was consistent with previous results.

Adsorption isotherm

The adsorption isotherm curves of various polymers are shown in Figure 5a. The saturated adsorption capacity of SMIPs (22.67 mg g^{-1}) was approximately twice that of the bulk MIPs (10.31 mg g^{-1}). The imprint factor ($IF = Q_{MIP}/Q_{NIP}$) of SMIPs was 6.3, which was about approximately three times that of the bulk MIPs (IF=2.2). This indicated the obvious dominance of SMIPs. Two commonly used isotherms, Freundlich and Langmuir, were employed in this study[39]. The plot $\ln q_e$ versus $\ln C_e$ was used to validate the linearised Freundlich isotherm, and the equation for SMIPs can be described as: y = 0.3873x+0.6168, with the correlation coefficient R^2= 0.9027 (Table 3). The plot $1/q_e$ versus $1/C_e$ was used to validate the linearised Langmuir isotherm. The equation for SMIPs can be described as: y = 0.039x + 4.3074, with the correlation coefficient R^2=0.9962, suggesting that the Langmuir model was more suitable for the experimental data than the Freundlich model because of the higher correlation coefficient. It suggests that the adsorption of SMIPs for PNLA was monolayer adsorption[43].

Adsorption kinetics

Kinetic modelling, which provides characteristics of possible reaction mechanisms, not only can estimate the adsorption rates but also makes it possible to optimise the rates[44]. As shown in Figure 5b, SMIPs and SNIPs reached adsorption equilibrium at 45 min; however, the bulk MIPs took twice as long (90 min) to reach adsorption equilibrium owing to the embedded activity site, indicating that the surface imprinted polymers facilitated the rebound of target molecules. The rapid mass-transfer rate of SMIPs is attributed to the most recognition sites at the surface or in proximity to the surface of SMIPs for easy diffusion of target analytes into imprinting cavities. This virtue is conductive to SMIPs being used as SPE sorbents.

Selectivity experiments

The binding specificity properties of the polymers with six different solute molecules were investigated (Figure 6). The *IF*s of SMIPs for oxiracetam, penicillin, benzoic acid, 6-aminopenicilanic acid, cloxcilloic acid and penicilloic acid were 1.0, 1.8, 2.0, 2.5, 2.6 and 6.3, respectively (Figure 7). The results indicated that SMIPs exhibited high selectivity towards PNLA versus other compounds. In the binding process, many specific recognition sites with respect to template molecule were generated on the surface of SMIPs, so PNLA was strongly bound to the surface imprinted polymers. As a non-homologue, oxiracetam had a distinct structure from PNLA, and the recognition sites of the imprinting cavities were not complementary to oxiracetam. Consequently, it had a smaller chance to be adsorbed onto the SMIPs. For the analogues, SMIPs presented some degree of adsorption capacity, especially for

CLA and 6-APA which are also the impurities in β-lactam antibiotics. These could be due to the similar structure or the identical functional group with PNLA. In contrast, the *IFs* of SMIPs for the four analogues were still lower than those for PNLA, and these fully confirmed that SMIPs had high specificity.

The selectivity of the SMIPs was specifically evaluated with the mixed solutions of PNLA and PENG at four concentration ratios. As shown in Figure 8, with the increase of the content of PENG, the competitive adsorption for PENG was slightly increased, and the selective factor (S=R_{PNLA}/R_{PENG}) fell off. The reason is that PENG had a greater chance than PNLA to approach the SMIPs at a high content of PENG, and so PENG hindered the access of PNLA to some extent. However, with a decrease in the content of PNLA, the adsorption ratio of SMIPs for PNLA was still gradually increased. Even at a ratio of 1:99, 92% of PNLA was absorbed by SMIPs, which indicated that SMIPs had high selectivity for PNLA.

Method validation

The chromatograms of the penicillin standard solution and penicillin mixed with PNLA were compared. A good separation was achieved between PENG and PNLA. The retention times of PNLA and PENG were 2.36 min and 6.19 min, respectively (Figure 9). The result indicated that this method could be used to detect PNLA in PENG solution. The limit of detection and quantitation (LOD and LOQ, respectively) in mixed solutions were calculated to be 0.03 mg g^{-1} and 0.1 mg g^{-1} for PNLA, respectively. The linearity of the calibration curve was evaluated for PNLA over the range of 0.1 to 50 mg g^{-1} in the penicillin solution with a correlation coefficient (r) =

0.998. The intra-day precision was evaluated by six repeated injections of each spiked standard (0.1, 1 and 10 mg g^{-1}). Similarly, the inter-day precision was examined by performing the assays on three consecutive days. The intra-day and inter-day precisions were consistent with the limit of 10% (Table 2). SMIPs-SPE columns had good recoveries (> 76%) for PNLA at various concentrations, indicating that this method could be used to detect PNLA in samples.

Reusability and stability of SMIPs-SPE

To evaluate the reusability and stability of SMIPs-SPE, the same SMIPs-SPE was reused eight times for binding/removing PNLA (10 $\mu g \cdot mL^{-1}$). When the SMIPs-SPE was repeatedly used eight times, the absolute recoveries of PNLA were all ≥75%, although the recovery of SMIPs-SPE decreases (Figure 10). This indicated that SMIPs-SPE had a good stability and reusability.

Application

As shown in Fig. 11(A), five batches of PENG samples were analysed by HPLC, and PNLA was not detected in all samples. Whereas, the content of PENG was different in the five samples, indicating that the quality of penicillin is uneven in China. The five batches of PENG samples were also analysed by SMIPs-SPE coupled with HPLC, and the results show that PNLA was also not detected in all samples, indicating that the five batches of PENG samples were qualified and they were also well preserved. However, one of benzylpenicillin sodium solution was detected with various placing times at room temperature, and the result is shown in Fig. 11(B). The results show that the content of penicillin was dramatically decreased with an increase

in the placing time; additionally, a portion of the penicillin was veritably decomposed to penicilloic acid. Almost all of the penicillin was degraded after placing for 10 days, and the content of penicilloic acid grew to 6%, suggesting that penicillin is likely to be decomposed to penicilloic acid during the procedure of production, improper storage, transportation and use of penicillin.

Conclusion

We describe a surface molecular imprinted polymer that offers high affinity, high concentration and specific recognition of PNLA by SMIPs-SPE. SMIPs offer special recognition towards the target molecular (PNLA) in contrast to the nonanalogue and several analogues. Moreover, SMIPs show a high absorption capacity and provide fast kinetics for PNLA. The SMIPs as new SPE sorbents can be used for the specific recognition of PNLA and extracting the penicilloic acid from the raw medicine of penicillin. Additionally, SMIPs-SPE has good stability and reusability. The SMIPs-SPE method coupled with HPLC was established to detect the trace amount of PNLA in penicillin, and the limit of detection is 0.03 $mg \cdot g^{-1}$, which is only one-third of the Maximum Residue Limit of each impurity in penicillin (MRL≤0.1 $mg \cdot g^{-1}$)[15-17]. To our knowledge, it is the first report that molecular imprinting technology is used for the control of the pharmaceutical impurities. The SMIPs-SPE could also prove highly useful in the separation and elimination of allergenic impurities in the manufacture procedure of penicillins. And this work could provide a promising method for the control of pharmaceutical impurities for the current pharmaceutical industry.

Acknowledgements

This work was financially supported by the National Natural Science Foundation of China (No. 81173024) and the National Key Projects of China (No. 812278063). We are grateful to Dr Min Zhang for revising the paper.

Reference

1 C.K.Pan, F.Liu and M.Motto, *J. Pharm. Sci*., 2011,**100**, 1228-1259.

2 V. F. Samanidou, E. N. Evaggelopoulou and I. N. Papadoyannis, *J. Sep. Sci.*, 2006, **29**, 1879-1908.

3 A. J. Apter, H. Schelleman, A. Walker, K. Addya and T. Rebbeck, *J. Aller. Clin. Immun*., 2008, **122**, 152-158.

4 E. Macy, R. J. Burchette. *Aller.*, 2002, **57**, 1151-1158.

5 E. Macy, P. K. Richter, R. Falkoff and R. Zeiger, *J. Aller. Clin. Immun*., 1997, **100**, 586-591.

6 B. B. Levine and A. P. Redmond, *Intern. Arch. Aller. Immun*., 1969, **35**, 445-455.

7 C. W. Parker, J. Shapiro, M. Kern and H. N. Eisen, *J. Exp. Med*., 1961, **115,** 821-838.

8 M. A. Schwarts, *J. Pharm. Sci*., 1969, **58**, 643-661.

9 B. B. Levine, *J. Exp. Med*., 1960, **112**, 1131-1156.

10 A. L. D. Weck and C. H. Schneider, *Immun*., 1968, **14**, 457-473.

11 A.Romano, *Aller*., 2007, **62**, 53-58.

12 A. L. D. Weck and H. N. Eisen, *J. Exp. Med*., 1960, **112**, 1227-1247.

13 SY Cai, CQ Hu and MZ Xu, *J. Pharm. Biomed. Anal*., 2003, **31**, 589-596.

14 D. J. Waxman and J. L. Strominger, *Ann Rev. Biochem*., 1983, **52**, 825-869.

15 European Pharmacopoeia Committee. European pharmacopoeia-7th Edition. European Directorate for Quality Medicines. 01/2008:0113.

16 Society of Japanese Pharmacopoeia. Japanese pharmacopoeia 16 edition. Society of Japanese Pharmacopoeia, 2011, 349.

17 China Pharmacopoeia Committee. Pharmacopoeia of the People's Republic of China. China Medical Science Press. 2010, 424.

18 A. D. Deshpande, K. G. Baheti and N. R. Chatterjee, *Curr. Sci*., 2004, **87**, 1684-1695.

19 E. Roets, P. Rappe, M. Heeren, J. Hoebus, A. Verbruggen and J. Hoogmartens, *J. Pharm. Biomed. Anal*, 1996, **14**, 1141-1149.

20 M.A.J. Van Opstal, R. Wolters, J. S. Blauw, P. C. Van Krimpen, W. P. Van Bennekom and A. Bult. *J. Pharm. Biomed. Anal*, 1990, **8**, 49-60.

21 M. Cole, M. D. Kenig and V. A. Hewitt, *Antimicr. Ag. Chemother*, 1973, **3,** 463-468.

22 J. Birner. *J. Pharm. Sci*, 1970, **59**, 757-760.

23 M. C. Hennio. *J. Chrom. A*, 1999, **856**, 3-54.

24 M. R. Halhalli, E. Schillinger, C. S. A. Aureliano and B. Sellergren. *Chem. Mat*, 2012, **24**, 2909-2919.

25 W. Du, Q. Fu, G. Zhao, P. Huang, YY. Jiao, H. Wu, ZM. Luo and C. Chang. *Food Chem*, 2013, **139**, 24-30.

26 R. Fernandez-Torres, M. Ol ás Consentino, M.A. Bello Lopez and M. Callejon

Mochon. *Talanta*. 2010, **81**, 871-880.

27 Y. Inoue, A. Kuwahara, K. Ohmori and H. Sunayama, *Biosens. Bioelec*, 2013, **48**, 113-119.

28 WH. Zhao, N. Sheng, R. Zhu, FD. Wei, Z. Cai, MJ. Zhai, SH. Du and Q. Hu. *J. Haza. Mat*, 2010, **179**, 223-229.

29 S. K. Tsermentseli, P. Manesiotis, A. N. Assimopoulou and V. P. Papageorgiou, *J. Chrom. A*, 2013, **1315**, 15-20.

30 H. Li, L.H. Nie, Y.N. Li, Z.H. Zhang, H. Shi, W.B. Hu and Y.K. Zhang. *Separa. Sci. Tech.*, 2009, **44**, 370-385.

31 H. Li, Y.J. Liu, Z.H. Zhang, H.P. Liao, L.H. Nie and S.Z. Yao. *J. Chrom. A*, 2005, **1098**, 66-74.

32 M. Shamsipur, H. R. Rajabi, S. M. Pourmortazavi and M. Roushani. *Spectro. Acta Part A: Mol. Biomol. Spectro*, 2014, **117**, 24-33.

33 G. Szekely, J. Bandarra, W. Heggie, F.C. Ferreira and B. Sellergren. *Separa. Puri. Tech.*, 2012, **86**, 190-198.

34 G. Szekely, J. Bandarra, W. Heggie, B. Sellergren and F.C. Ferreira. *Separa. Puri. Tech.*, 2012, **86**, 79-87.

35 J. M. Pan, H. Hang, X. H. Dai, J. D. Dai, P. W. Huo and Y. S. Yan. *J.Mat. Chem*, 2012, **22**, 17167-17175.

36 Y. M. Yin, Y. P. Chen, X. F. Wang, Y. Liu, H. L. Liu and M. X. Xie. *J. Chrom. A*, 2012, **1220**, 7-13.

37 I. Ghebre-Sellassie, S. L. Hem and A. M. Knevel. *J. Pharm. Sci*, 1984, **73**,

125-128.

38 W. J. Cheng, Z. J. Liu and Y. Wang. *Talanta*, 2013, **116**, 396-402.

39 G. F. Malash, M. I. El-Khaiary. *J. Coll. Interf. Sci.*, 2010, **348**, 537-545.

40 D.K. Singh, S. Mishra. *Desalination*. 2010, **257**, 177-183.

41 British Pharmacopoeia Volume I & II, Monographs: Medicinal and Pharmaceutical Substances, Benzylpenicillin Sodium. British Pharmacopoeia 2009, (Ph Eur monograph 0113)

42 ICH-International Conference on Harmonisation of Technical Requirements for Registration of Pharmaceuticals for Human Use (2005). Validation of analytical procedures: Text and methodology Q2 (R1). In ICH Expert Working Group, ICH Harmonised Tripartite Guideline (pp. 1-13). Geneva.

43 O. M. Akpa, E. I. Unuabonah. *Desalination*, 2011, **272**, 20-26.

44 A. Heidari, H. Younesi, Z. Mehraban and H. Heikkinen. *Inter. J. Bio. Macromol*, 2013, **61,** 251-263.

Figure Captions:

Figure 1 The Schematic representation of the route for the synthesis of SMIPs

Figure 2 SEM images of activated silica gels (a,d), SNIPs (b,e) and SMIPs (c,f) with various magnifications

Figure 3 FTIR spectra of activated silica gels (a), APTES-SiO_2 (b), MIPs (c) and SMIPs (d)

Figure 4 TGA curves of activated silica gels (a), APTES-SiO_2 (b), SMIPs (c) and SNIPs (d)

Figure 5 (a) Adsorption isotherm curves of SMIPs, SNIPs and MIPs; (b) Adsorption kinetic curves of SMIPs, SNIPs and MIPs

Figure 6 (a) Molecular structures of PENG, PNLA, 6-APA, benzoic acid, Cloxcilloic acid and Oxiracetam; (b) Mass spectrum of penicilloic acid

Figure 7 The adsorption of the polymers for six different solute molecules

Figure 8 The adsorption ratio of PNLA and PENG and the selective factors of various concentration ratio (C_{PNLA}:C_{PENG})

Figure 9 HPLC chromatograms of PENG (a) and PENG spiked with PNLA (b); 1: PNLA; 2: PENG

Figure 10 Recoveries of PNLA on recycling SMIPs-SPE

Figure 11 (A) The chromatograms of benzylpenicillin sodium for injection. (a) blank; (b) penicilloic acid; (c~g) benzylpenicillin sodium for injection Ⅰ~Ⅴ. (B) The chromatograms of penicillin aqueous solution with various placing times. (a) 10 days; (b) 8 days; (c) 5 days; (d) 3 days; (e) 2 days; (f) 1 day; (g) 0 day; (h) the chromatograms of penicilloic acid solution

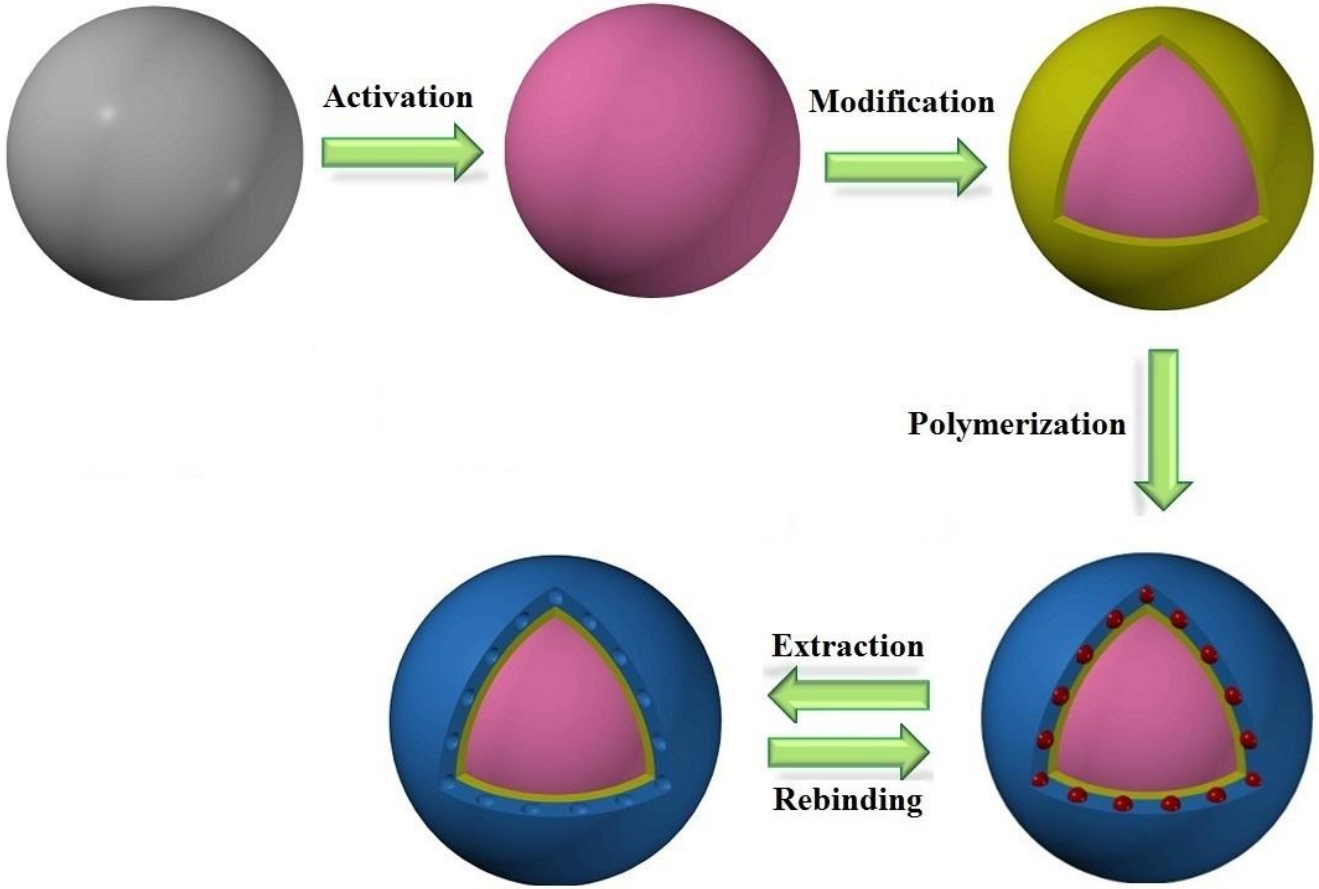

Figure 1

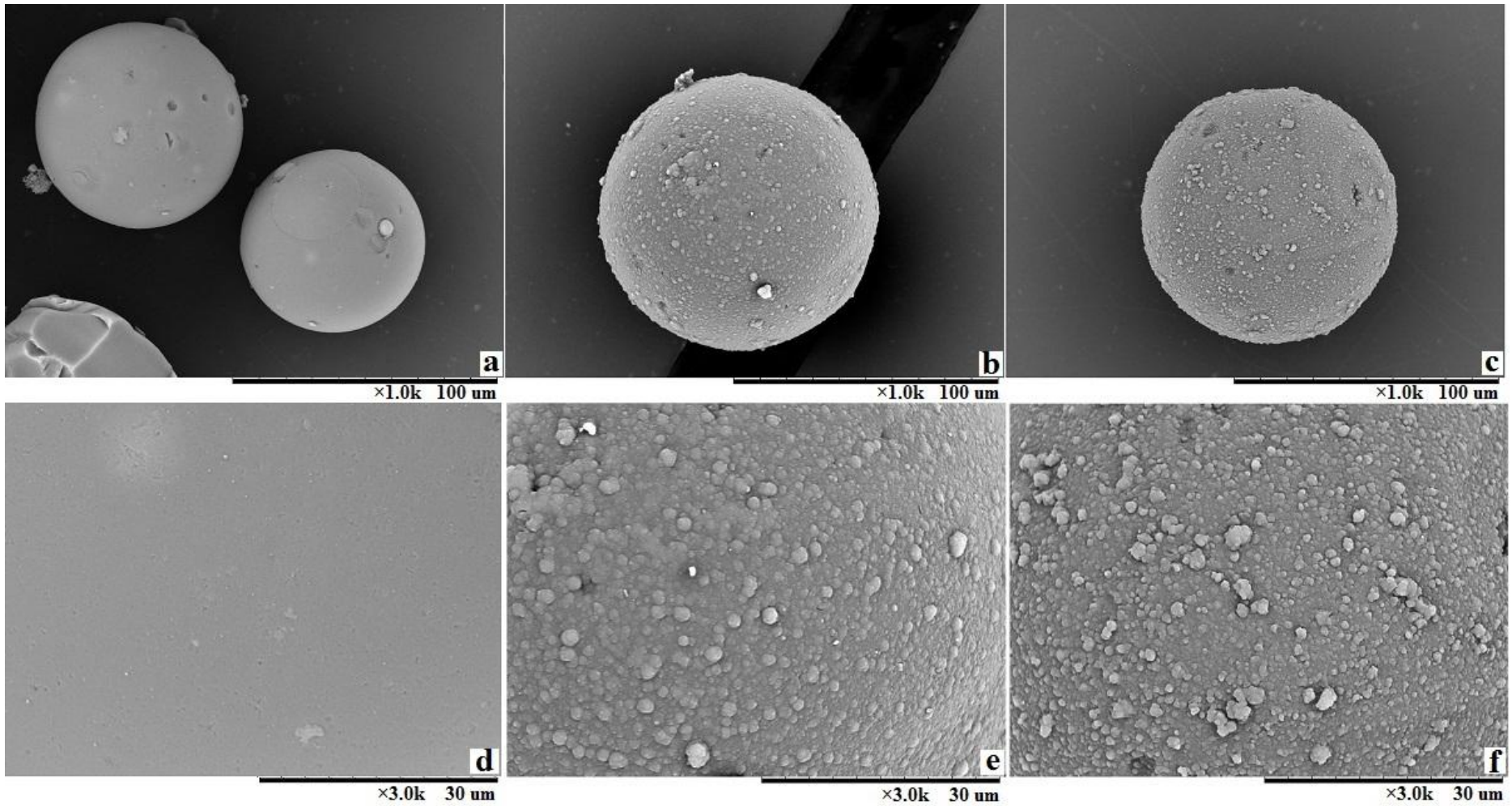

Figure 2

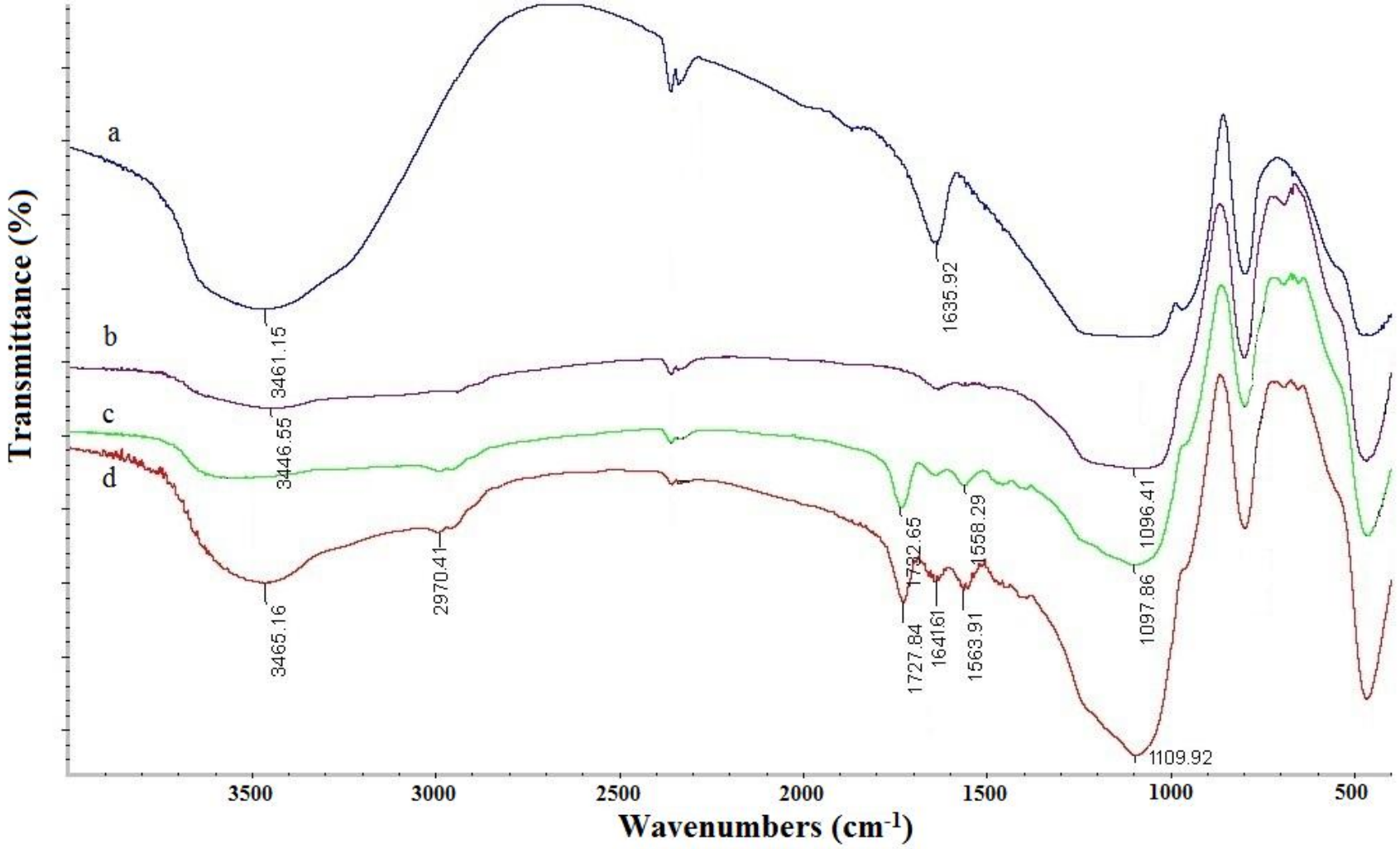

Figure 3

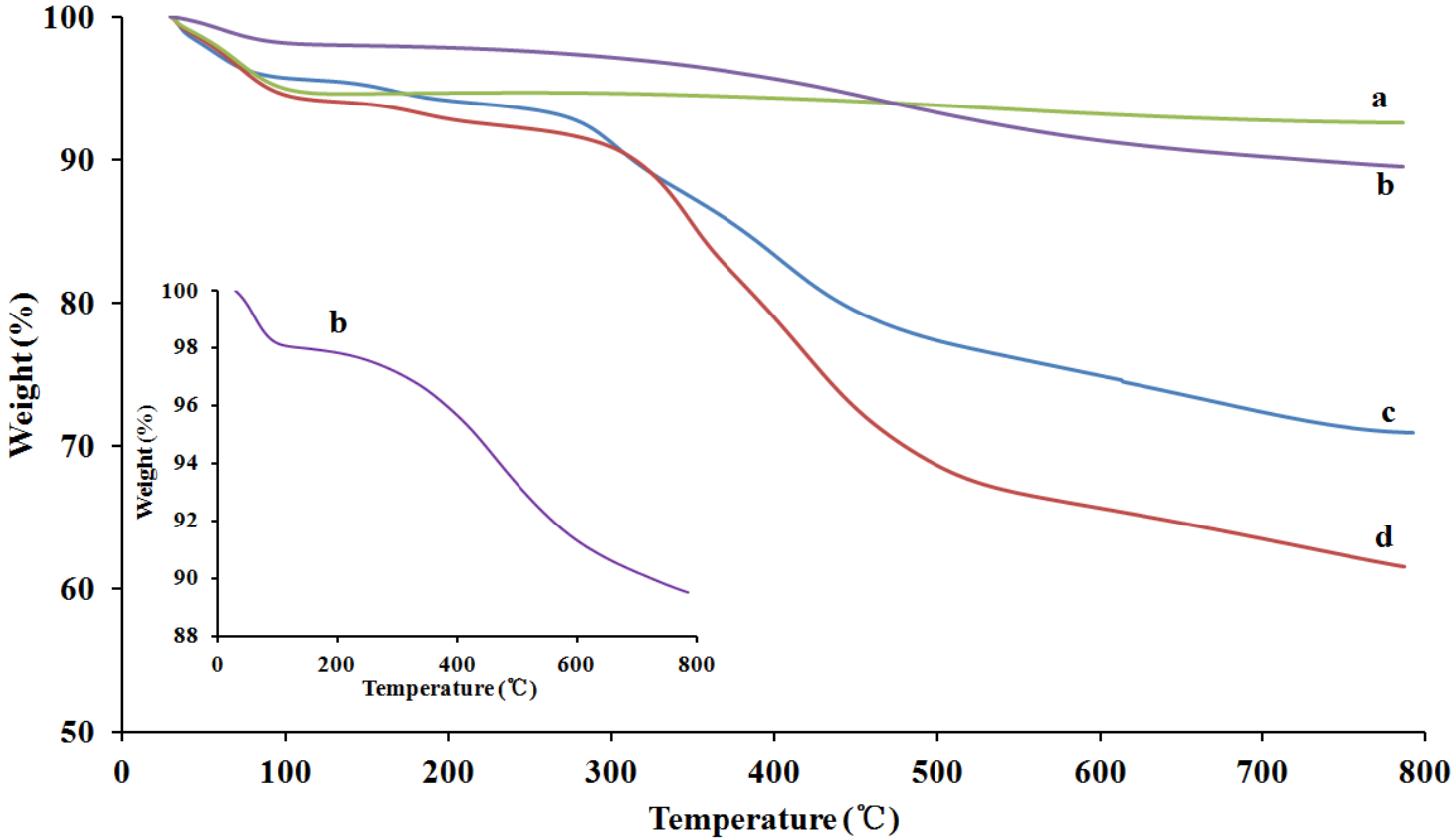

Figure 4

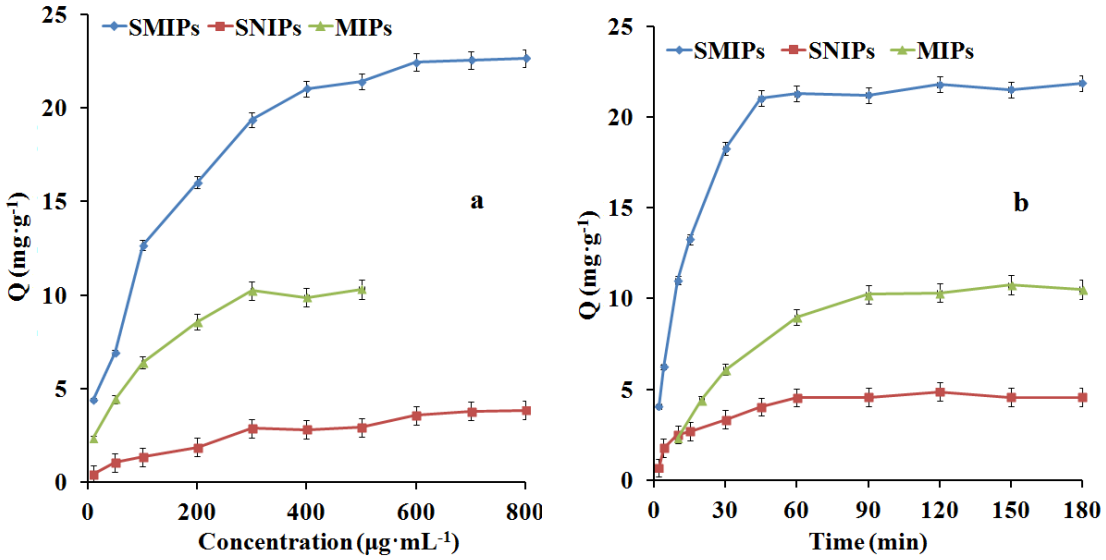

Figure 5

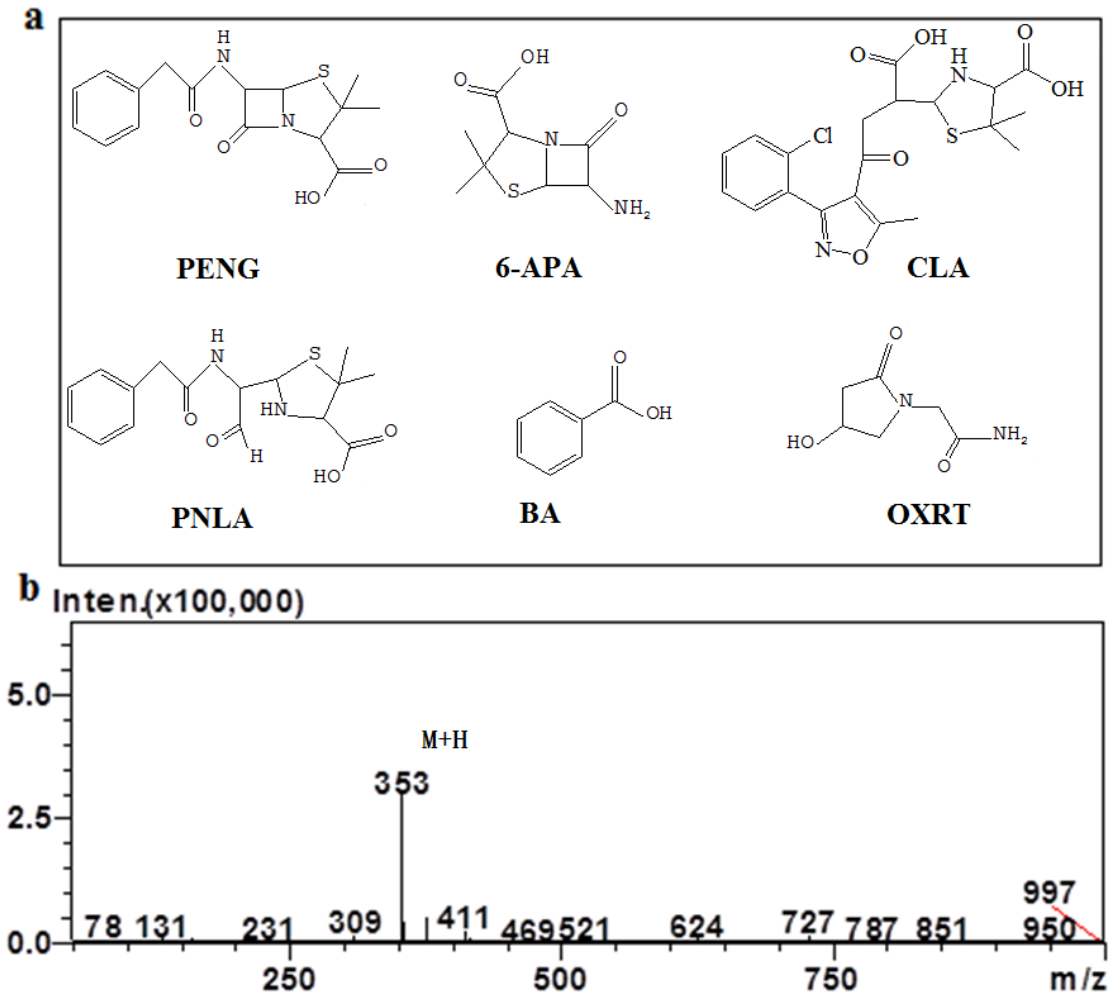

Figure 6

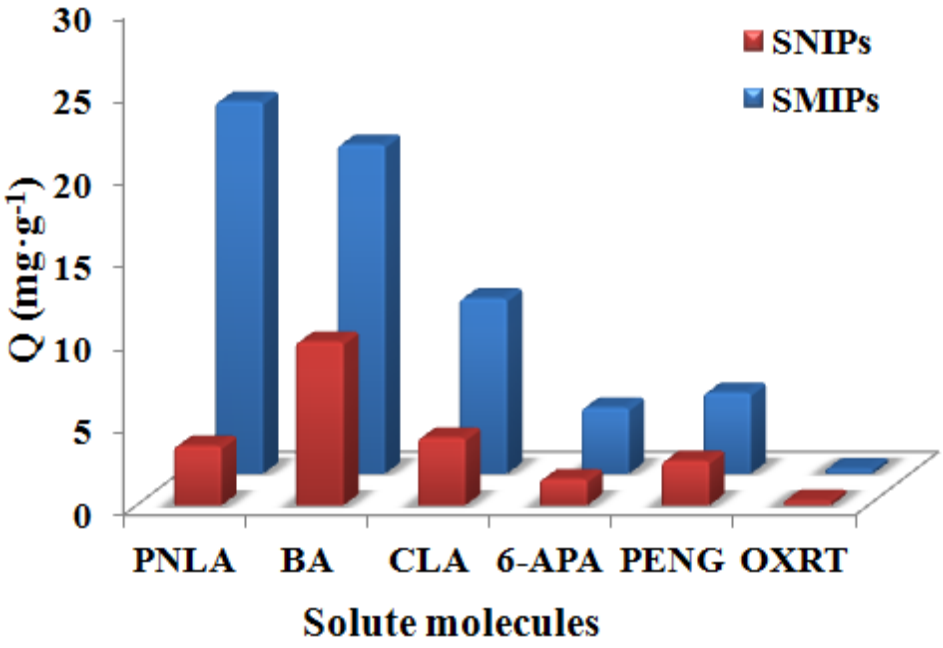

Figure 7

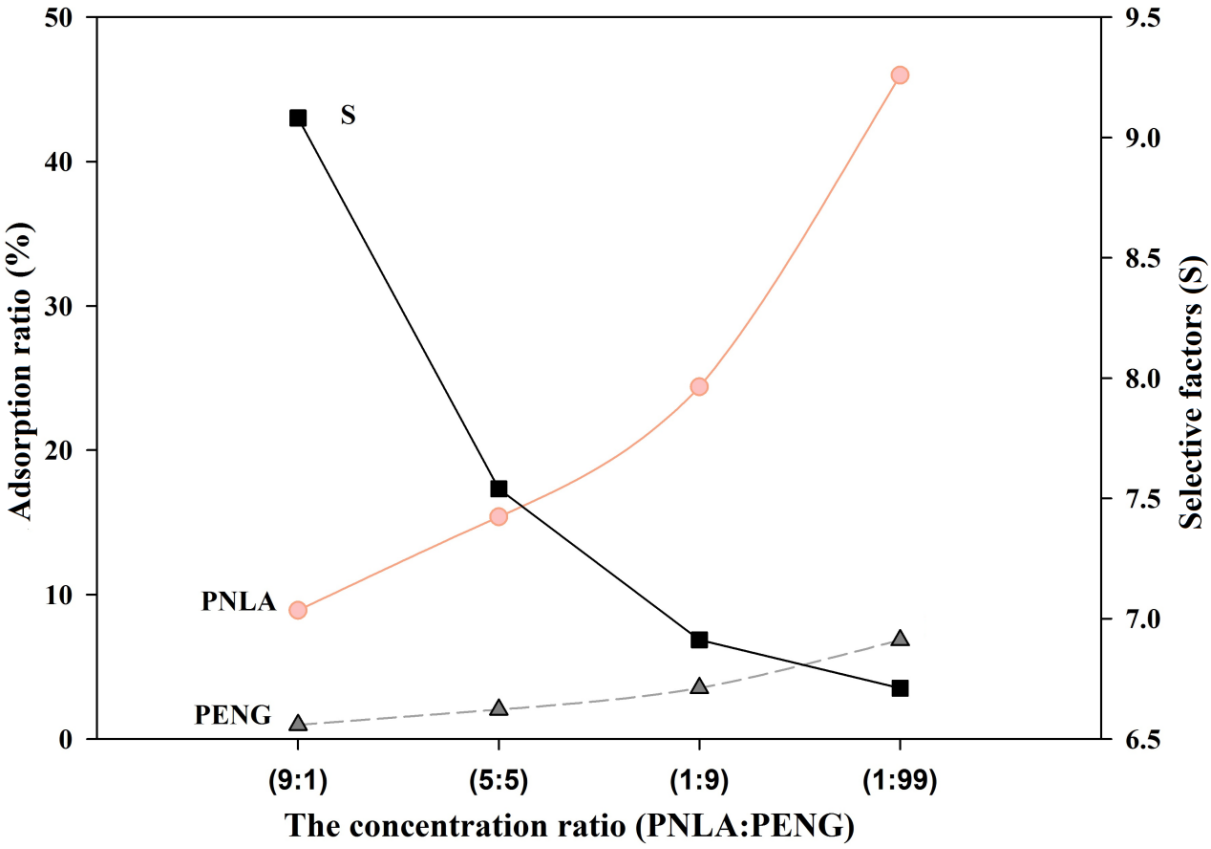

Figure 8

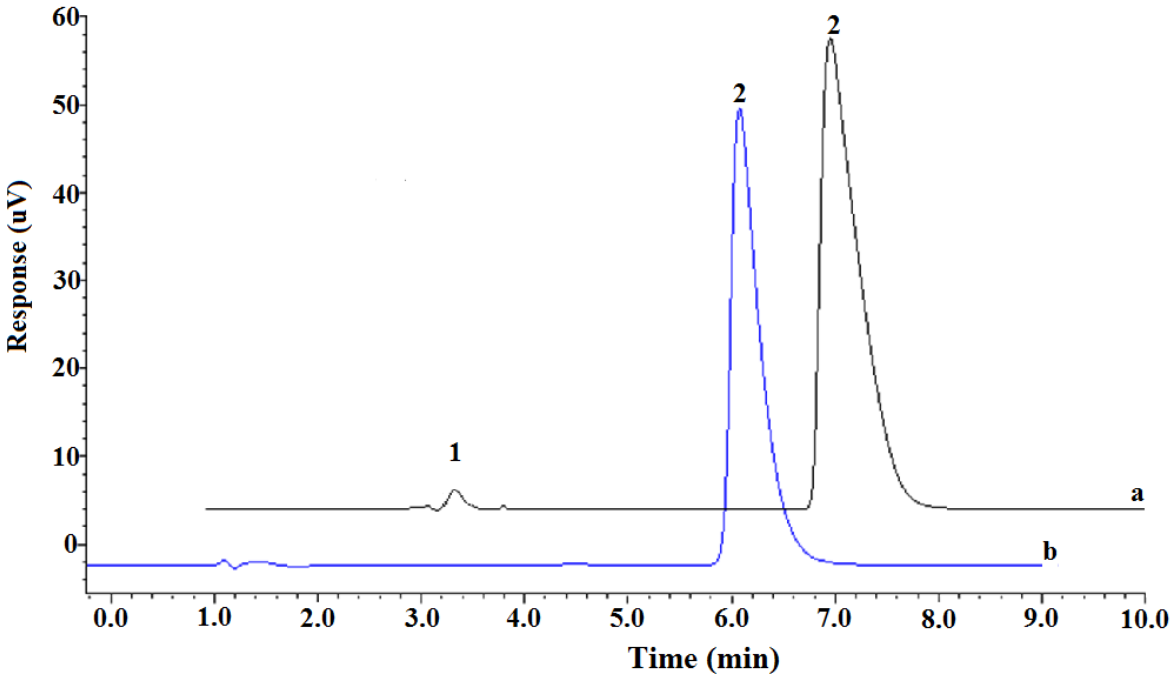

Figure 9

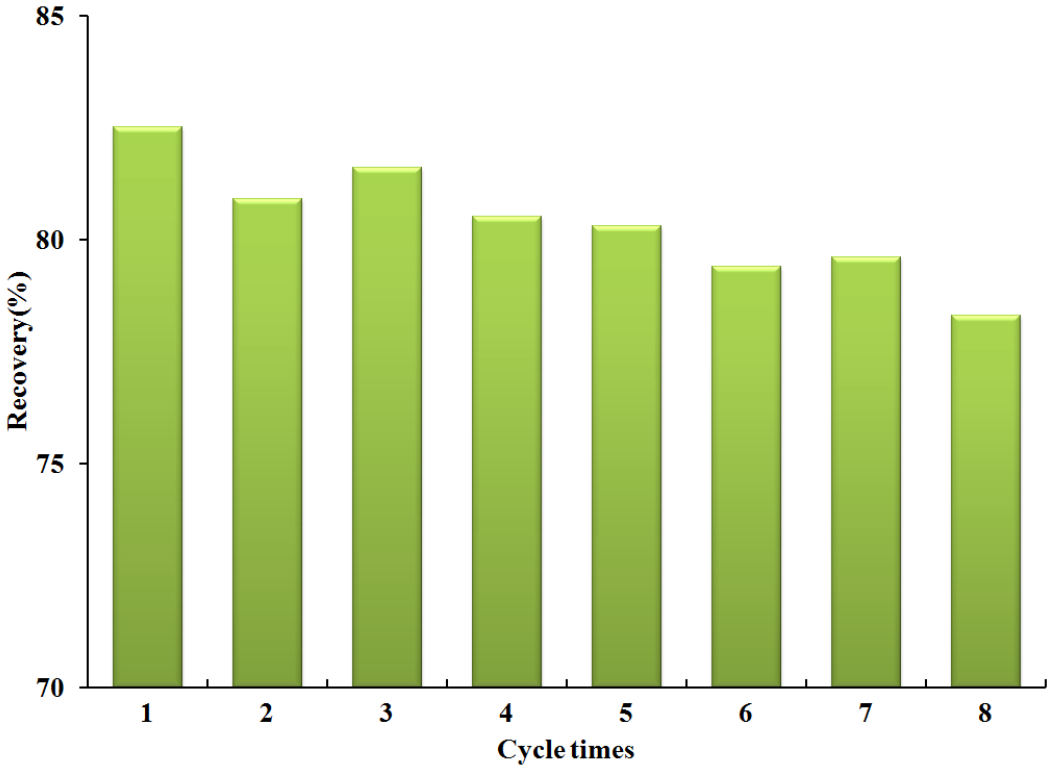

Figure 10

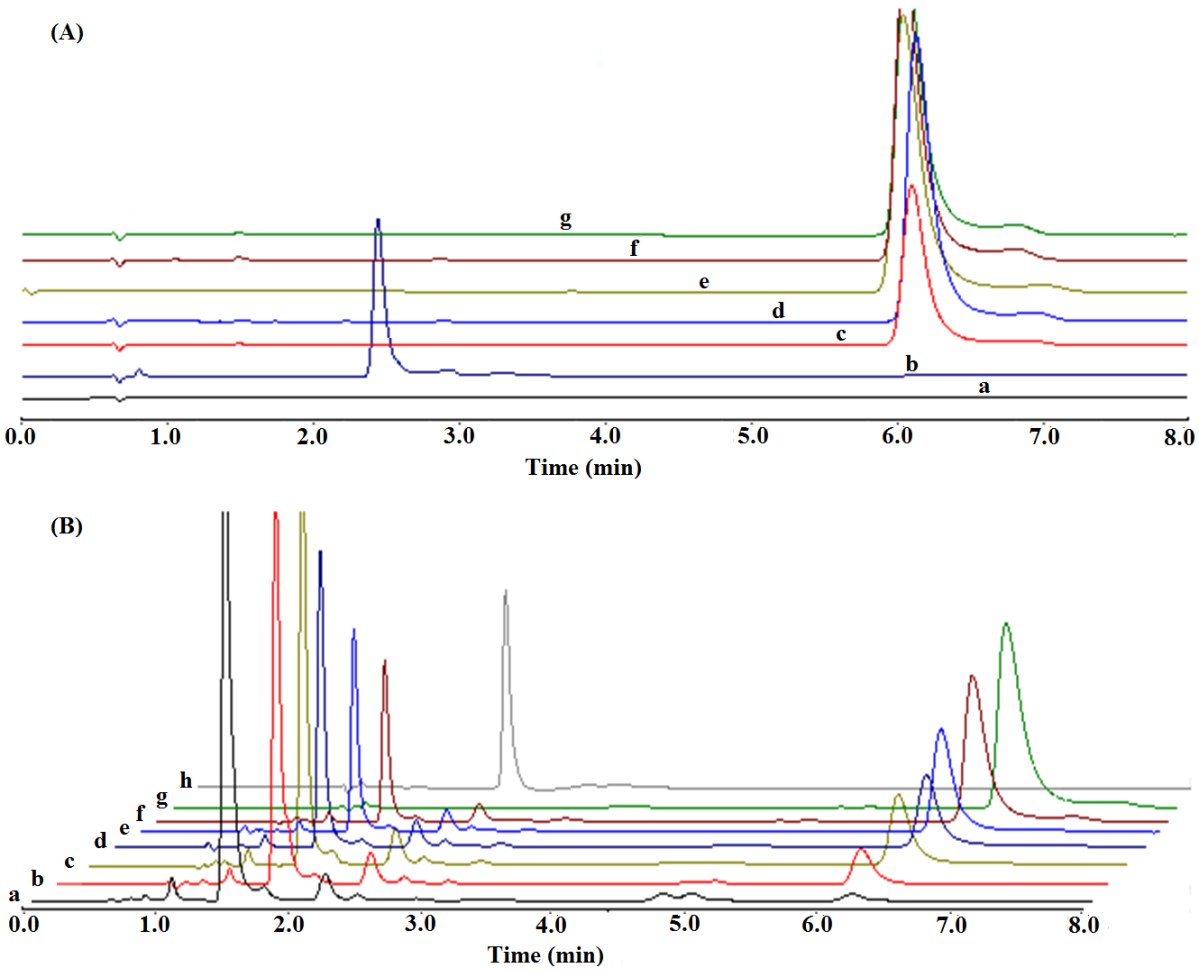

Figure 11

Table 1 Nitrogen adsorption/desorption analysis and elemental analysis

Sample	$C^{(a)}$ (%)	$N^{(a)}$ (%)	$D^{(a)}$ ($\mu mol \cdot (m^2)^{-1}$)	Coverage$^{(a)}$ (%)	$d^{(a)}$ (nm)	$d_L{}^{(a)}$ (nm)	$S^{(b)}$ ($m^2\ g^{-1}$)	$d_p{}^{(b)}$ (nm)	$V_p{}^{(b)}$ ($mL\ g^{-1}$)
Activated silica	0	0	/	/	/	/	407.35	6.74	0.84
APTES-SiO_2	5.81	2.11	1.28	15.96	0.35	1.14	/	/	/
SMIPs	15.71	1.61	3.35	41.82	2.17	0.70	264.22	4.93	0.41
SNIPs	20.21	1.63	4.57	57.13	3.13	0.60	236.18	4.28	0.29

(a) Obtained from elemental analysis; (b) Obtained from nitrogen adsorption/desorption analysis;

Table 2 Accuracy and precision

Sample	Concentration ($mg \cdot g^{-1}$)	Intra-day(n=6)		Inter-day(n=3)		Recovery (%)	RSD (%)
		Accuracy (%)	Precision RSD (%)	Accuracy (%)	Precision RSD (%)		
PNLA	0.1	93.2	6.8	94.5	5.2	76.2	8.1
	1	94.6	1.1	92.3	7.4	79.0	6.9
	10	95.1	0.7	90.9	4.9	88.3	7.6

Table 3 The parameters of Freundlich and Langmuir models for the adsorption of PNLA onto SMIPs

Freundlich isotherm			Langmuir isotherm		
K_f	n	R^2	q_m(mg·g^{-1})	K_a(L·mg^{-1})	R^2
1.85	2.58	0.9027	25.64	0.1679	0.9962